July 13, 2025

We thank both reviewers for their second review of the manuscript and for recommending the paper for publication. We are pleased that most of the initial comments from the reviewers were addressed in the revised manuscript. Two further edits have been made to address the remaining comments from both reviewers, which are detailed below.

1. First, we agree with the second reviewer that the analysis of the baseline case at different Strouhal numbers is a worthy result for publication, and it has been included in the revised manuscript. In particular, Figure 1 of this document is now discussed at the beginning of Section 3, and then the remainder of the results focus in on $St = 0.3$, as this corresponds to the dominant frequency in the baseline wake and the selected AWC forcing frequency.

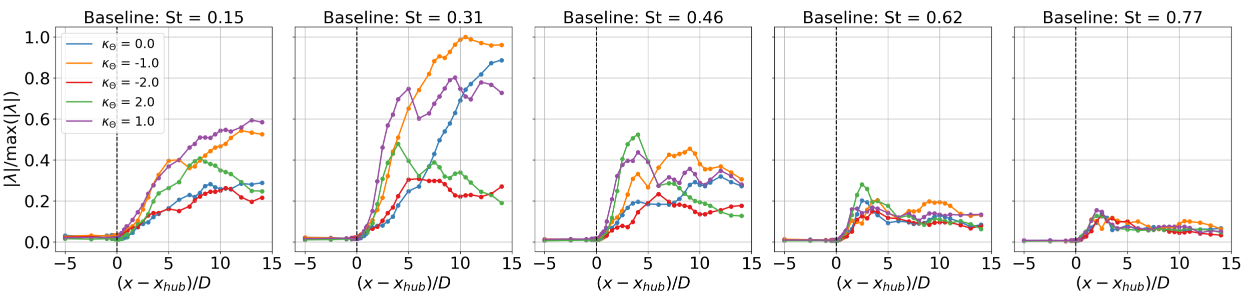

Figure 1: Eigenvalues of **S** at five different Strouhal numbers for the baseline case. Shown are the azimuthal wavenumbers $\kappa_\theta = 0$ (—), $\kappa_\theta = 1$ (—), $\kappa_\theta = -1$ (—), $\kappa_\theta = 2$ (—), and $\kappa_\theta = -2$ (—). Each eigenvalue is normalized by the global maximum baseline eigenvalue across all streamwise locations and Strouhal numbers.

The utility of SPOD for identifying the optimal AWC forcing frequency *a priori* based on baseline wake data is also suggested, and the authors feel that a more detailed investigation of wind turbine wakes within the range $St \in [0.25, 0.35]$ across different atmospheric conditions would be worthwhile for future research. We note that the SPOD parameters selected in this study do not permit for such fine resolution.

Please see the latest version of the manuscript for the revised text, highlighted in blue.

2. Second, it seems the analysis of the two-turbine array presented in Section 3.3 has caused some confusion and we apologize for the miscommunication. Upon revisiting the paper after a few months, we agree with the second reviewer that the analysis of power and loads for different pitching amplitudes does not align well with the primary focus of the manuscript, which centers on $A = 1.25°$. Additionally, the results at $A = 0.5°$ and $2°$ may introduce questions that detract from the overall narrative of the paper.

However, we do believe there is a value in connecting the spectral analysis of turbine loads, wake TKE, and turbulent entrainment that is discussed in the preceding sections to practical quantities of interest, specifically the power gains of a downstream turbine and conventional loading metrics for the upstream turbine.

Therefore, we considerably streamlined the discussion in Section 3.3. Figures 22 and 23 have been combined into a single figure (see Figure 2 in this document), which focuses exclusively

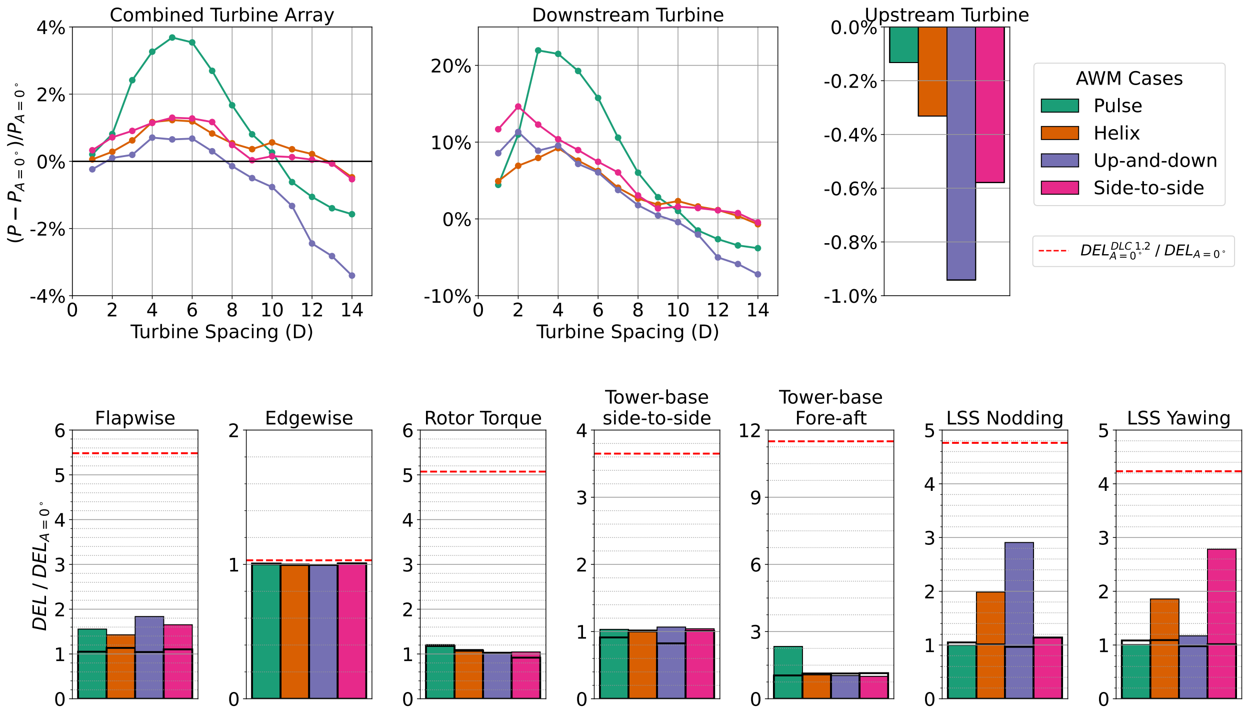

Figure 2: (top) Percent change in generated power, P, from the baseline case ($P_{A=0^\circ}$) for a two turbine array with the turbine spacings ranging from $1D$ to $14D$. The results for the upstream turbine are computed from the LES, while the downstream turbine results are obtained from a stand-alone OpenFAST simulation using YZ-planes from the LES as inflow data at each streamwise location. AWM is applied to the upstream turbine with $A = 1.25^\circ$, while the downstream turbine is operated using baseline controls. (bottom) Baseline-normalized damage equivalent loads (DEL) for seven different load channels. Solid bars indicate DELs for the upstream turbine, while the DELs for the turbine $5D$ downstream are outlined in black. The red dashed line corresponds to the DELs of the turbine using baseline controls in DLC 1.2 conditions (single seed) derived from the Normal Turbulence Model with a hub height wind speed of 6.4 m/s (i.e., turbulence intensity of 25.90%).

on the two-turbine array results for the $A = 1.25^\circ$ cases. In this figure, the change in power from the baseline case is shown for the two-turbine array, as well as for the downstream and upstream turbines individually. Moreover, the DELs for seven different load channels are also shown for the upstream turbine and a downstream turbine. Note, in the revised manuscript, DELs are shown for a turbine spaced $5D$ downstream, as this corresponds to the location where the combined power increase is maximized. In addition to the revised figure, the discussion in this section has been significantly shortened to focus on the main cases of interest.

Even though the $A = 0.5^\circ$ and $A = 2^\circ$ results are no longer included in the manuscript, we would still like to respond to the reviewers comments about these cases to the best of our ability. The three main comments about this section are discussed below:

- Power gains for the helix at $A = 0.5^\circ$: We do not have a great explanation yet for the small increase in power observed for the helix case at small pitching amplitudes. The first reviewer may be correct that this is due to a lack of statistical convergence for the $A = 0.5°$ LES cases. However, we would like to note that this trend is something that we have occasionally observed in other simulations when using small pitch amplitudes, even with different turbine models and wind conditions. Nonetheless, more work is needed to understand if this result is significant or not, and so we have decided to omit these findings from the current manuscript.

- Loss in power for the up-and-down case at $A = 2.0°$: The reviewer correctly notes that the up-and-down case loses more power than the other strategies at $A = 2°$, even producing less power than the baseline for the two turbine array. We believe this is a result of the airfoil operating in a suboptimal region of the lift curve when a large pitching amplitude is applied to the turbine blade in the vertical $0°$ position. The vertical position is where the angle-of-attack is typically near its maximum, especially in the presence of a highly sheared inflow. A similar discussion can be found in the work of Taschner et al. [2023].
- Changes in reported values: The reviewers are correct that a few numerical values in Section 3.3 have changed from the original version of the manuscript. In the initial version, a slightly different averaging window was applied to all the AWC cases and the baseline case. Specifically, given a time series of data on the interval $t \in [t_0, t_1]$, the following averaging windows were initially used for all cases:

$$\begin{aligned}
\text{Baseline} &: t \in [t_0, t_1] \\
\text{Pulse} &: t \in [t_0, t_0 + \lfloor (t_1 - t_0)/(2\pi/\omega_e) \rfloor \times 2\pi/\omega_e] \\
\text{Helix} &: t \in [t_0, t_0 + \lfloor (t_1 - t_0)/(2\pi/(\bar{\Omega} - \omega_e)) \rfloor \times 2\pi/(\bar{\Omega} - \omega_e)] \\
\text{Side-to-side} &: t \in [t_0, t_0 + \lfloor (t_1 - t_0)/(\pi/\omega_e) \rfloor \times \pi/(\omega_e)] \\
\text{Up-and-down} &: t \in [t_0, t_0 + \lfloor (t_1 - t_0)/(\pi/\omega_e) \rfloor \times \pi/(\omega_e)]
\end{aligned}$$

  where $\omega_e = 2\pi St U_\infty / D$ is the excitation frequency, and $\bar{\Omega}$ is the mean rotor speed. This approach was taken to closely match the period of oscillation or the "beat-envelope" of each AWC case, as described by Cheung et al. [2024]. However, this difference in the averaging window led to inconsistencies when comparing AWC cases and in the reported baseline-normalized values, especially in the presence of a non-uniform inflow, which was not an issue in [Cheung et al., 2024]. Moreover, one of the numerical values was not updated correctly in the revised text. In the current manuscript, we have ensured that the power and DEL results reported in Section 3.3 are averaged over seven equal Strouhal periods after the transients from the stand-alone OpenFAST simulations are discarded, and this information is included in the text. Averaging over an equal number of Strouhal periods accounts for the large fluctuations in power introduced by the pulse method [Frederik et al., 2020] while also ensuring consistency in the time intervals across cases.

Please see the latest version of the manuscript for the revised text, highlighted in blue, and note that much of the text in Section 3.3 has been removed from earlier versions.

References

Lawrence C Cheung, Kenneth A Brown, Daniel R Houck, and Nathaniel B deVelder. Fluid-dynamic mechanisms underlying wind turbine wake control with strouhal-timed actuation. Energies, 17 (4):865, 2024.

Joeri A Frederik, Bart M Doekemeijer, Sebastiaan P Mulders, and Jan-Willem van Wingerden. The helix approach: Using dynamic individual pitch control to enhance wake mixing in wind farms. Wind Energy, 23(8):1739–1751, 2020.

Emanuel Taschner, Aemilius AW van Vondelen, Remco Verzijlbergh, and Jan-Willem van Wingerden. On the performance of the helix wind farm control approach in the conventionally neutral atmospheric boundary layer. In Journal of Physics: Conference Series, volume 2505, page 012006. IOP Publishing, 2023.